

14-10
N 9 2 - 3 3 3 6 9
P 10

THE MEASUREMENT SYSTEM OF PULSE MODULATED CARRIER FREQUENCY STABILITY AND TIMING JITTER

Li Cheng - Fu

Beijing Institute of Radio Metrology and Measurement

P.O. Box: 3920 Beijing, China

Abstract

This paper describes the definition of pulse modulated carrier frequency stability and timing jitter as well as the configuration and synchronous acquisition measurement method of its measurement system.

Frequency stability of pulse modulated carrier is measured with discrimination technique. The pulse modulated carrier under test is mixed with a reference frequency synthesizer. A delay line is used to convert the frequency fluctuation mixed IF signal to the voltage fluctuation. The system has the capability to make the phase noise measurement of two port devices on pulsed carrier using phase bridge.

The noise voltage mentioned above is applied to the data acquisition and processing unit by pc to realize stability measurement. The data acquisition is in the form of pulse synchronization so that the measurement system accuracy is increased. The pulse width is more than 0.3 μ s. The phase fluctuation variance σ is less than 0.017.

The time interval measuring system with high resolution is used to make interpulse timing and pulse width jitters automatic measurement. The pulse width is less than 0.2 ns. The resolution is 0.1 ns. The system is successfully applied to radar measurement.

INTRODUCTION

The frequency stability is one of the important qualifications of signal source.

Characterization and measurement of CW frequency stability already have been matured and united. But there is still no unanimity in characterization of the carrier frequency stability on pulsed wave for the time being. An application of pulse wave to the radar on the other hand is urgently needed.

The duty cycle of pulse modulated wave is smaller in general. The signal frequency spectrum is more complex. This causes difficulty on characterization and measurement.

The CW method has been used to measure pulse modulated carrier frequency stability.

Measurement and characterization of pulse modulated carrier frequency stability using this method can cause the following problems. At first, the general pulse repeat frequency rate is lower. The RF pulse sideband spectrum line is a lot and dense. Pulse noise sophistication resulting from these factors stated above makes Fourier band noise be band is $\frac{f_p}{2}$.

Because of the same cases, Allan variance does not fit to characterize frequency stability in time domain.

The other question is to acquire very small video frequency impulse train of duty cycle. By CW acquisition, forming a lot of acquired data is useless.

The acquired data in the pulse width only is useful, and acquisition can also leak. The smaller the duty cycle, the greater the leakage rate. The confidence of measured results is degraded.

It is only adapted to measurement under the condition of higher duty cycle. The duty cycle required in general $\frac{\tau}{T}$ is larger than 5% (to test source), $\frac{\tau}{T} > 1\%$ (to test dual-port devices) [6].

Using the synchronization data acquisition technique proposed in this paper, we have solved the measurement problem of lower duty cycle.

This system has the capability to make frequency stability measurement of dual-port device on pulse modulated carrier. The microwave mixed IF discrimination technique is used to test pulse modulated carrier frequency stability.

Measurement of interpulse timing jitter is accomplished with analog interpolation and precision time measurement technique.

I. CHARACTERIZATION FOR FREQUENCY STABILITY ON PULSE MODULATED CARRIER

To measure pulse modulated carrier frequency stability may use for reference of CW characterization and measurement method in principle.

Our proposed methods are: to characterize frequency stability in time domain using interpulse variance, and to characterize phase noise sophistication efforts according to difference and practical necessary requirement between CW band pulse modulated wave.

1. Characterization of Pulse Modulated Carrier Frequency Stability in Time Domain

Change in the statistical rate of pulse modulated carrier series adjacent in pulse modulated carrier described by interpulse variance may be written as:

$$\sigma^2 = \langle (F_1 - F_2)^2 \rangle \quad (1)$$

When we determined with the measurement system in Figure 1, A/D converter output is a form of pulse repeat frequency at a rate as a separate digital time series, can be written as

$$\sigma^2(N.T.\tau) = \frac{1}{N-1} \sum_{i=1}^N [\Delta f(i) - \Delta f(i-1)]^2 \quad (2)$$

Where T = Pulse period
 τ = Pulse width
 N = Measurement number of each group
 $f\Delta(i)$ = Average value of frequency fluctuation is 1th pulse.

2. Characterization of Pulse Modulated Carrier Frequency Stability in Frequency Domain

Assume,

unmodulated carrier $f_1(t) = A \cos \omega_c t$ (3)

pulsed waveform $f_2(t) = \frac{\tau}{T} \left(1 + \sum_{i=1}^{\infty} \frac{\sin n \omega_p \frac{\tau}{2}}{n \omega_p \frac{\tau}{2}} \right)$ (4)

pulse modulated signal $f_3(t) = f_1(t) \times f_2(t)$ (5)

$$f_3(t) = A \cdot \frac{\tau}{T} \cos \omega_c t + A \cdot \frac{\tau}{T} \sum_{n=1}^{\infty} \frac{\sin \omega_p \frac{\tau}{2}}{n \omega_p \frac{\tau}{2}} [\cos(\omega_c + n \omega_p)t + \cos(\omega_c - n \omega_p)t] \quad (6)$$

the spectrum corresponding with equation (6) is shown in Figure 5.

The corresponding spectral density of phase fluctuation may be expressed as

$$S'_{\phi}(f) = A \frac{\tau}{T} S_{\phi}(f) + A \frac{\tau}{T} \sum_{n=1}^{\infty} \frac{\sin n \omega_p \frac{\tau}{2}}{\omega_p \frac{\tau}{2}} [S_{\phi}(f + n f_p) + S_{\phi}(f - n f_p)] \quad (7)$$

When ignoring the effect of the sample function, the equation (7) may be simplified as

$$S'_{\phi}(f) = A \frac{\tau}{T} \sum_{n=-\infty}^{\infty} S_{\phi}(f + n f_p) \quad (8)$$

the influence of spectrum superimpose to $S_{\phi}(f)$ is calculated to $S'_{\phi}(f)$ in equation (8)

The magnitude of the superimposition phase noise is corresponding with the following:

(a) When τ is fixed, the spectral density and supimposition of phase noise are increased with a decrease of f_p .

- (b) When f_p is fixed, the superimposition of phase noise is becoming worse, with the narrow of τ .
- (c) If $S_{\phi}(f)$ is composed of a broken line, $S_{\phi}(f)$ will become the level line. If $S'_{\phi}(f)$ is a monotone increasing or decreasing curve, $S'_{\phi}(f)$ is level line approximately. [5]

II. SYSTEM CONSTRUCTION AND OPERATION PRINCIPLE

1. Additive Phase Noise Measurement

The measurement of pulse modulated Carrier phase fluctuation can be realized by using the measurement principle of microwave phase bridge shown in Figure 1. The CW signal is divided into two path signals through a power splitter. The signals form a pulse modulated carrier wave throughout the PIN modulator, respectively.

One of them passed device under test is applied to RF port of the phase detector; another passed the phase shifter is applied to the LO port of the phase detector.

We can make a dual-channel signal to quadrature by means of adjusting the phase shifter. When the electronic length of two path signals is equal, the phase noise of the source is cancelled, because of the correlation act while the DUT phase noise is detected.

When the phase detector shown in Figure 1 is in quadrature, the output voltage of the phase detector is:

$$\Delta V(t) = K_{\phi} \sin \omega_p(t) \quad (9)$$

When

$$\Delta \Phi_{mix} \ll 1 \text{ rad,}$$

$$\Delta V(t) = K_{\phi} \cdot \Delta \Phi(t) \quad (10)$$

where K_{ϕ} = sensitivity of phase detection.

Thus, phase fluctuation under test of device is converted to voltage fluctuation $\Delta V(t)$. In measurement of phase fluctuation $\Delta \Phi(t)$ in time domain,

$$\Delta \Phi(t) = \frac{\Delta V(t)}{K_{\phi}} ,$$

RF pulse series, interpulse variance σ_p is given by data acquisition system as in Figure 4, and we can get $S'_{\phi}(f)$ or $\mathcal{L}'(f)$ through FFT.

The common source having lower phase noise is required in order to assure the measurement of the system having low phase noise bottom, at the same time the correlation of the measurement system is required in order to reduce the contribution of common source to output noise.

2. Interpulse Frequency Fluctuation Measurement

The measurement principle of interpulse frequency fluctuation is shown in Figure 2. Operation models of the system are single - channel and dual channel.

At first, IF is mixed up microwave signal. When using operation model of dual-channel, we can use IF quadrature dual-channel discrimination frequency system with a delayer as the frequency discriminator to measure pulsed carrier frequency fluctuation. It is fitted in with the source (transmitter) to measure large

frequency fluctuation. When using single channel operation model, the two path signals are applied to Q phase detector,

$$V_L(t) = A_1 \cos[\omega_0 t + \varphi_1 + \varphi(t)] \quad (11)$$

$$V_R(t) = A_2 \cos[\omega_0(t - \tau_1) + \Phi(t - \tau_1)] \quad (12)$$

Where, τ_1 = delay time, Φ_1 = shift of phase shifter, when two signals phase applied to phase detector are quadrature, detector output is

$$\Delta V(t) = \frac{1}{2} A_1 A_2 K \sin[\Phi(t) - \Phi(t - \tau_1)] \quad (13)$$

average frequency fluctuation in $(t, t - \tau_1)$

$$\Delta \omega = \frac{1}{\tau_1} \int_{t-\tau_1}^t \Phi'(t) dt = \frac{\Phi(t) - \Phi(t - \tau_1)}{\tau_1} = \Delta \omega = 2\pi \Delta f \quad (14)$$

when $\Delta \Phi(t) = \Phi(t) - \Phi(t - \tau_1) \ll 1$ rad, (14) formula is substituted for (13) we can get:

$$\Delta V(t) = K_\phi \cdot 2\pi \tau_1 \cdot \Delta f = K_d \cdot \Delta f \quad (15)$$

where $K_d = 2\pi \tau_1 K_\phi$ as frequency discriminator constant.

3. Data Acquisition and Processing Unit

Figure 4 is a block diagram of a data acquisition and processing unit.

The output signal of phase fluctuation $\Delta \Phi(t)$, frequency fluctuation $\Delta f(\tau)$ is shown in Figure 1. Figure 2 is converted to discrete digital signal with a high speed A/D converter.

It works by a pulse controlled under test. In interpulse, high speed acquisition is carried to receive useful information.

The disadvantage of continuous sample is overcome. The system is controlled by a computer through STD bus.

4. Time Fluctuation Measurement

The measurement of pulse width and timing jitter is accomplished by a counting unit with the analog interpolation under computer-control. The system has high accuracy and resolution. The measurement principle is shown in Figure 3.

III. MEASUREMENT RESULTS

The pulse width of system measurement can be narrowed down to $0.3 \mu s$, interpulse phase fluctuation variance value σ is less than 0.017. Frequency fluctuation σ is less than 50 Hz, timing jitter variance is less than 0.2 ns, the resolution is 0.1 ns. This system has an application in measurement of radar transmitting. The measured pattern is shown in Figure 6 and Figure 7.

REFERENCES

- [1] "Characterization of Frequency Stability" IEEE. Trans. on IM Vol. 1. 20, No. 2, May 1971.
- [2] Stanley, J. Goldamn, "Phase Noise Analysis in Radar System Using Personal Computers", 1990.
- [3] A. P. Rodis, "Phase Noise, Post and Telecommunication, 1988, Beijing.
- [4] John M. Milan, "Test Set for the Measurement of Transmitter Stability Parameters", Pro. 29th Annual Frequency Control Symposium, 1975.
- [5] Guo Yan Yin, "Frequency Stability of Modern Electronic Equipment" Astronautic Publishing House, 1989, Beijing.
- [6] "Pulse Carrier Phase Noise Measurement Using the HP3048A Phase Noise Measurement System", Hewlett-Packard Company, Feb 6, 1990.
- [7] Liu Xiafan and Mao Ruida, "An Automatic Measurement System for RF Pulse Stability Parameters", 20th PTTI, 1988.

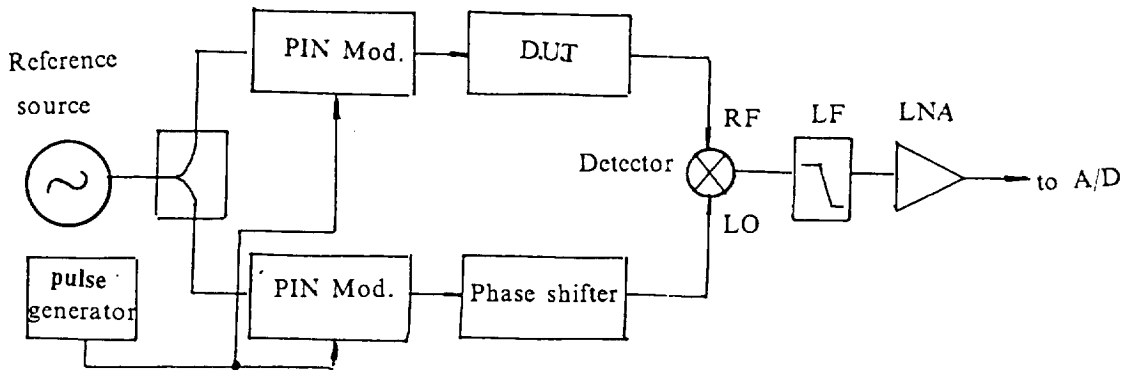


Fig.1 Additive phase noise measurement

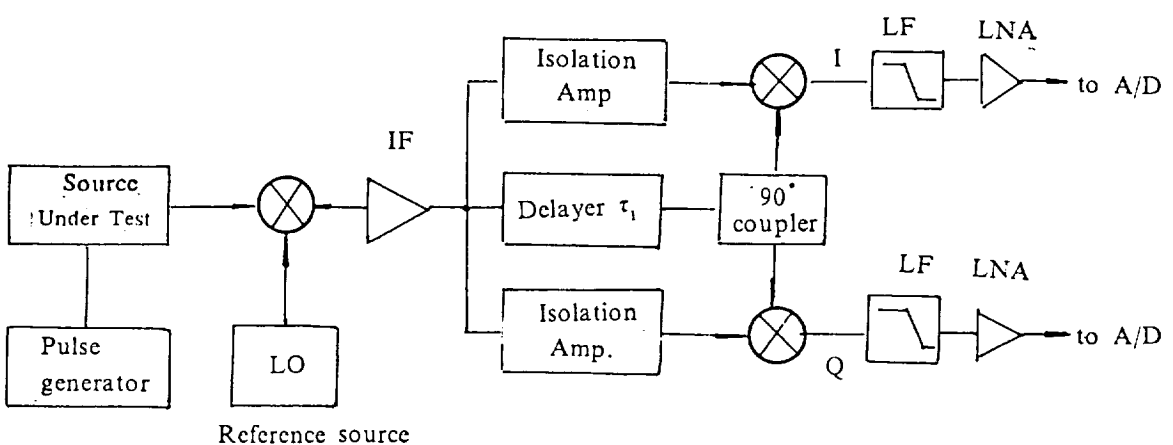


Fig.2 Measurement principle of frequency fluctuation

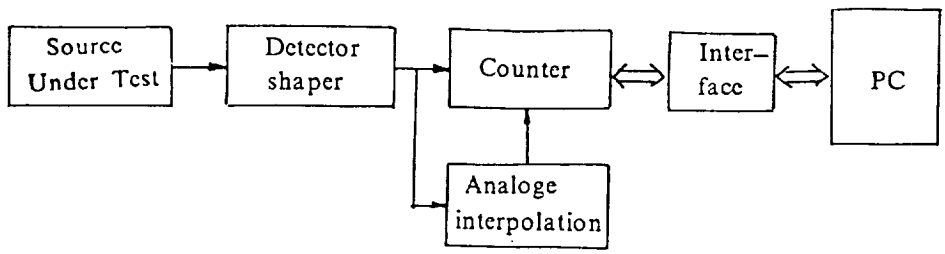


Fig.3 Time interval measurement

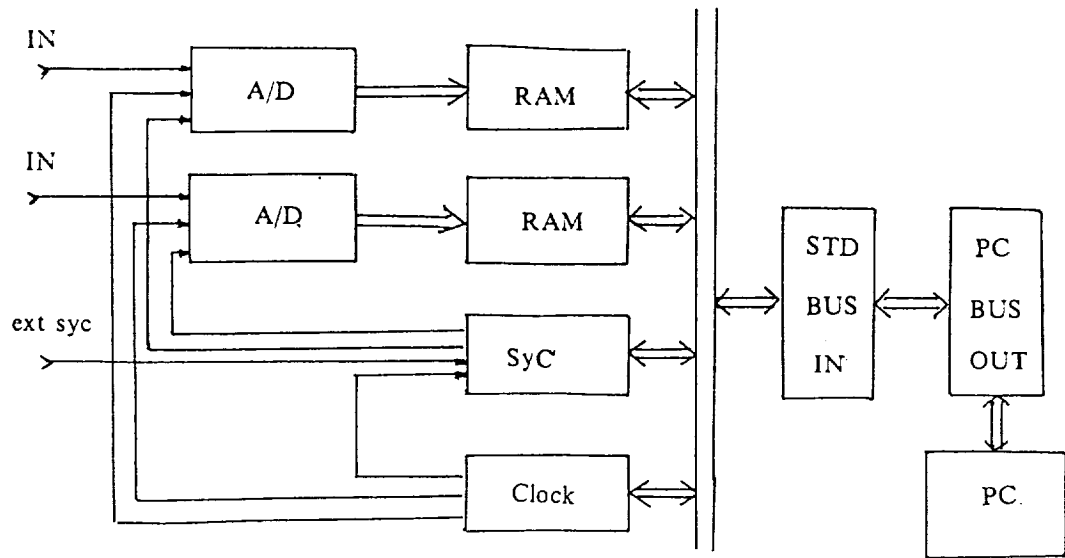


Fig.4 Data acquisition and processing unit

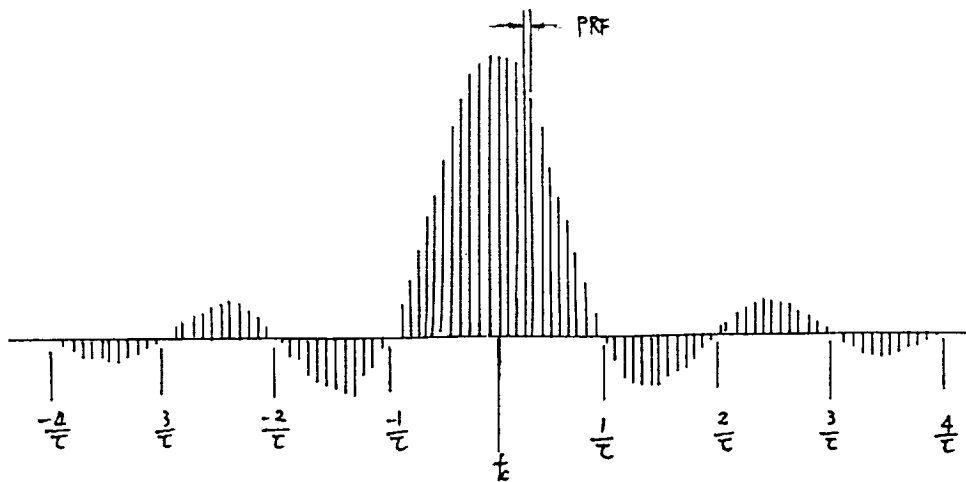


Fig.5 Frequency spectrum of pulse modulation carrier

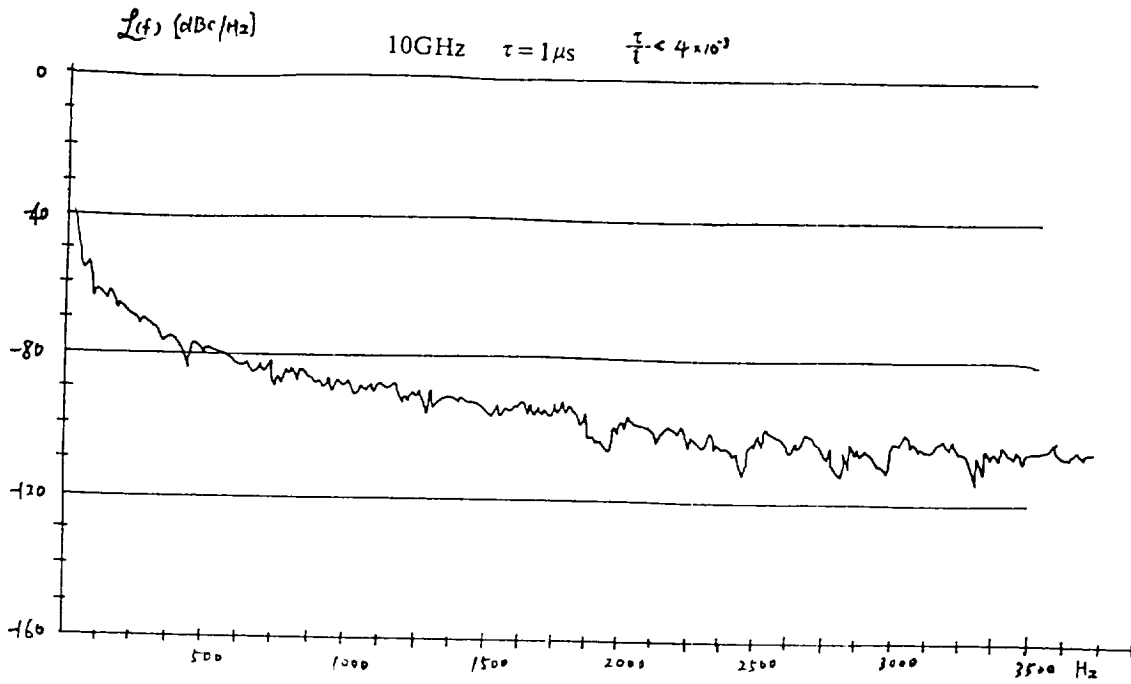


Fig.6 Radar TWT Amp. phase noise

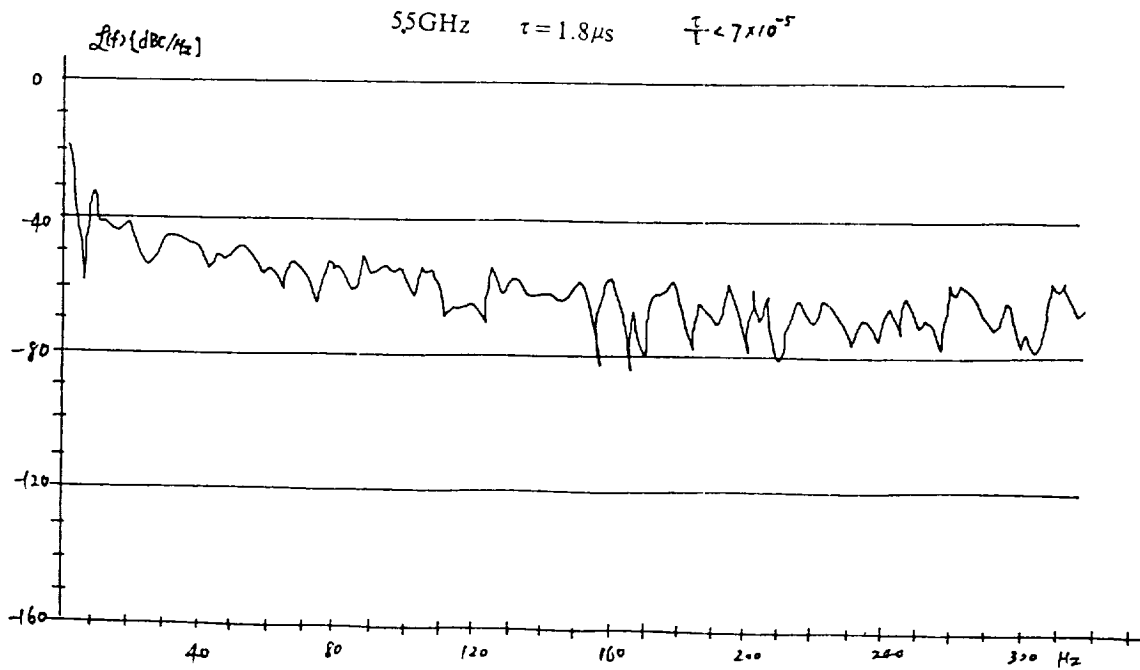


Fig.7 Radar transmitter source phase noise

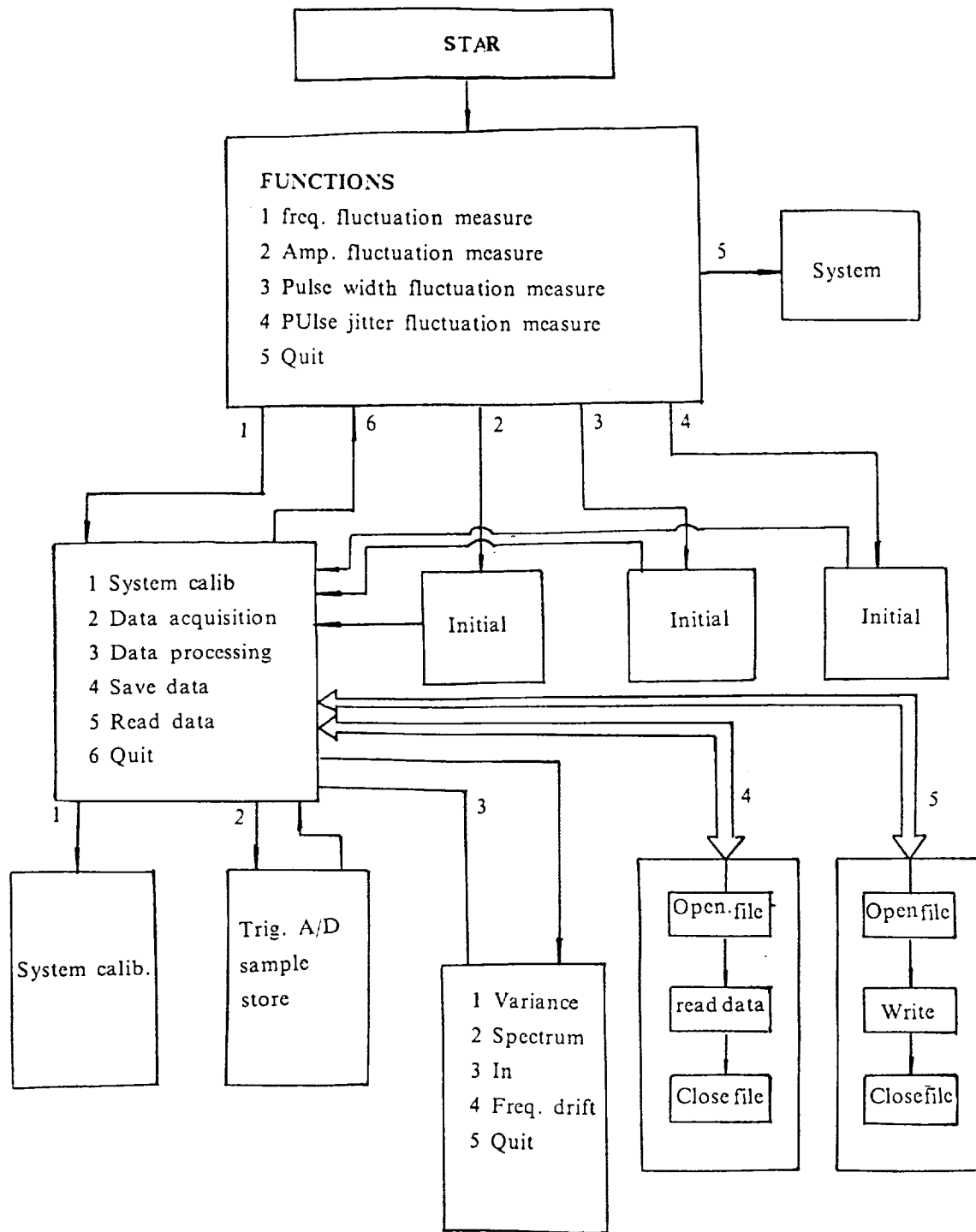


Fig.8 Flow chart of program